Design and fabrication of an integrated polarized light guide for liquid-crystal-display illumination

Ko-Wei Chien and Han-Ping D. Shieh

An integrated polarized light guide was designed and fabricated for use as a liquid-crystal backlight with emphasis on uniformity of the light and conversion of *p*-polarized to *s*-polarized light. Two different micro-optical structures were fabricated both on the top and the bottom surfaces of the light guide. On the top surface, a subwavelength grating separates *s*-polarized and *p*-polarized light to achieve a polarization-conversion efficiency of 69%. A 1.7 gain factor of polarization efficiency was obtained to increase the utility of light for liquid-crystal illumination. © 2004 Optical Society of America

OCIS codes: 260.1440, 150.1950.

1. Introduction

As applications for thin-film transistor liquid-crystal devices increase, bright and uniform backlight modules become essential. The optical efficiency of conventional backlight modules is low because there is no conversion of *p*-polarized to *s*-polarized light. In addition, the complex requirements for assembling optical films such as brightness enhancement films and dual brightness enhancement films and diffusers are usually not conducive to compact packaging. Many methods to separate *s*- and *p*-polarized light to produce singly polarized light to enhance polarization-conversion efficiency have been reported.[1] The wire grid polarizer is the simplest device that produces polarized light: An unpolarized electromagnetic wave impinges upon a grid of parallel conducting wires. The electric field can be decomposed into two orthogonal components, one of which is parallel and the other perpendicular to the wires. The field parallel to the wires drives the electrons along each wire and thereby heats the wires, thus transferring energy from the field to the grid. In contrast, the electrons are not free to move in the orthogonal direction, and the corresponding field is then propagated through the grid. However, more than 50% of incident light is absorbed by the grid of wires. Therefore a conventional wire grid polarizer is not efficient. A polarized light guide based on selective total internal reflection (TIR) at microgrooves for polarization conversion has also been proposed.[2] Anisotropic foil with diamond-turned microgrooves is filled with an isotropic index-matching layer that is attached to the light guide's substrate. The extraordinary optical axis is parallel to the groove direction. Therefore, only the field parallel to the groove direction is coupled out by TIR at the microstructure interface. The orthogonal field is not coupled out because the corresponding critical angle is sufficiently small and TIR is not present at the interface. Theoretically, the gain factor of polarization efficiency can be as high as 2. The approach of using the TIR that occurs in microgrooved anisotropic foil achieves a gain factor of polarization efficiency of 1.7.[2] However, the smoothness requirements of microgroove surfaces for reducing scattered light are stringent. Plastic particles are easily attached to microgroove surfaces during diamond turning. Thus, difficulty in fabrication of microgrooves hinders application of a polarized backlight module. Utilization of the Brewster angle of incidence to separate polarized rays was also proposed.[3] For unpolarized incident light, only the field perpendicular to the incident plane (*s*-polarized light) is reflected. However, polarization-separation efficiency decreases rapidly when the incident angle differs from the Brewster angle. The incident angle is critically limited. Use of the Brewster angle reduces the gain factor to only ~1 because *p*-polarized light is not recycled or converted to *s*-polarized light.

A novel integrated light guide for backlight mod-

K.-W. Chien (dodu.eo88g@nctu.edu.tw) and H.-P. Shieh (hpshieh@mail.nctu.edu.tw) are with the Institute of Electro-Optical Engineering, National Chiao Tung University, Hsinchu 30010, Taiwan.

Received 26 August 2003; revised manuscript received 2 December 2003; accepted 8 December 2003.

0003-6935/04/091830-05$15.00/0

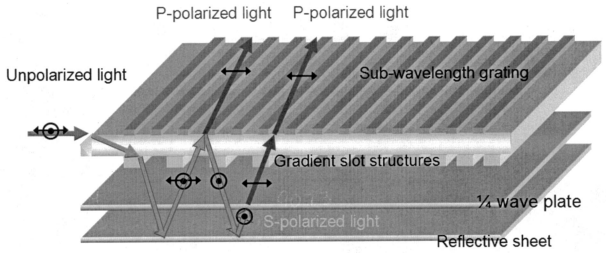

Fig. 1. Schematic of an integrated light guide. P-polarized light is transmitted and *s*-polarized light is reflected. S-polarized light is then converted into *p*-polarized light by passing through a quarter-wave plate twice.

ules was designed to achieve polarization conversion and compactness for liquid-crystal device illumination, as shown in Fig. 1.[4] When unpolarized light was coupled to the light guide, slot structures on the bottom surface coupled light out of the guide. Light was then reflected by a reflective sheet. When the subwavelength grating impinged on the top surface, only *p*-polarized light was transmitted while *s*-polarized light was reflected. *s*-polarized light was then converted into *p*-polarized light by passing twice through a quarter-wave plate. The subwavelength grating is not critically dependent on incident angle. The 75% efficiency of the subwavelength grating degraded to 10% if the incident angle varied by ±20°. Therefore, outcoupled light was singly polarized, as was required for LCD illumination.[5]

2. Method of Operation

The light guide model (8.8 cm wide and 7.1 cm long) was built by use of an optical simulation program to optimize the pattern design. Slot structures and a subwavelength grating were fabricated on the bottom and the top surfaces, respectively, of the light guide. On the bottom surface the slot structures were spaced with a greater gradient density in the region far away from the light source and less density close to the light source. As shown in Fig. 2, when the light source was coupled into the light guide by the slanted surface, obliquely incident guided rays were coupled out by the sidewalls of the slot structures. The slot structures determined the amount of outcoupled light, and therefore the density of slot structures controlled the uniformity of the outcoupling plane. A brightness profile of the outcoupling plane was obtained by ray tracing, as shown in Fig. 3. With a 650-lm white-light source, the maximum and minimum values of illuminance were 43,000 and 34,000 lux, respectively. The luminous efficiency increased from an average value of 18% to 31%. Uniformity of illuminance on the outcoupling plane can be as much as 80%, which is greater than the 70% uniformity required for a commercial light guide.

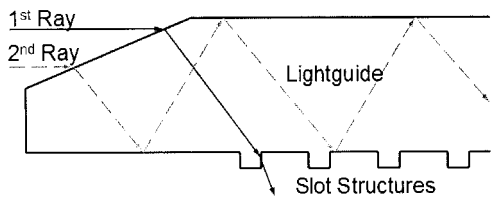

Fig. 2. Light source coupled into the light guide by a slanted surface. The oblique-incidence guided rays were coupled out by the sidewalls of the slot structures. The density of slot structures controlled the illuminance uniformity of the outcoupling plane.

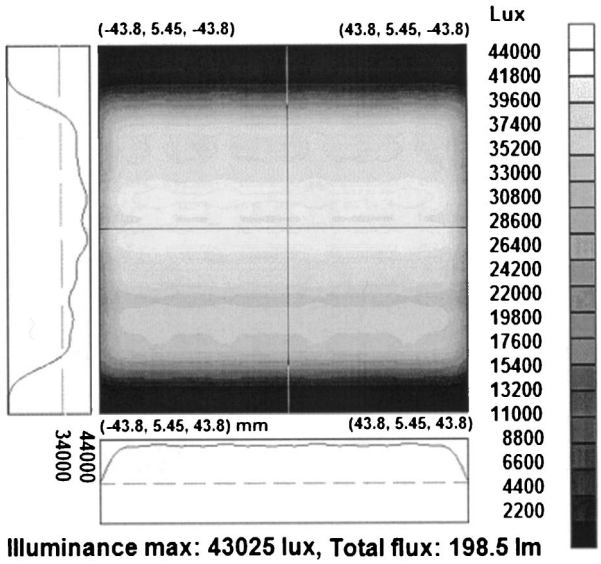

Fig. 3. Illuminance profile of the integrated light guide. The maximum and minimum values of illuminance were 43,025 and 34,000 lux, respectively. Consequently, 80% of uniformity was achieved.

Moreover, the operation of a subwavelength grating is based on the combined effects of form birefringence and the multilayer structure. If period Λ of the grating is sufficiently small compared with the wavelength, the whole structure behaves as if it were homogenous and uniaxially anisotropic, which are the attributes of form birefringence.[6] Orthogonally polarized light encounters different effective refractive indices because of the asymmetric grating structure. One polarization is parallel to the grating (*s*-polarized light) and the other is perpendicular to the grating (*p*-polarized light). Consider a one-dimensional grating composed of two materials of refractive indices n_1 and n_2 with duty cycle f; the effective indices are given by[7]

$$n_{\parallel} = [f n_1^2 + (1 - f) n_2^2]^{1/2}, \quad (1)$$

$$n_{\perp} = n_1 n_2 [f n_2^2 + (1 - f) n_1^2]^{-1/2}. \quad (2)$$

Similarly to the operational principles of a wire grid polarizer, unpolarized light was incident upon a metallic grating. The first diffracted order, which was linearly polarized in the direction perpendicular to the grating bar (*p*-polarized light), was designed to transmit through the subwavelength grating. In contrast, the zeroth diffracted order, which was linearly polarized in the direction parallel to the grating bar (*s*-polarized light) was reflected.[8] The subwave-

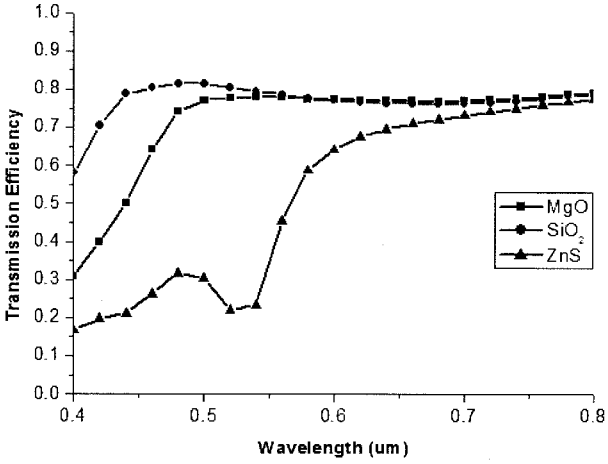

Fig. 4. Transmission efficiency of p-polarized light as a function of the wavelength of incident light for various materials of an additional dielectric layer. The period of the Al grating (100 nm thick) was 0.2 μm, with a 50% duty cycle.

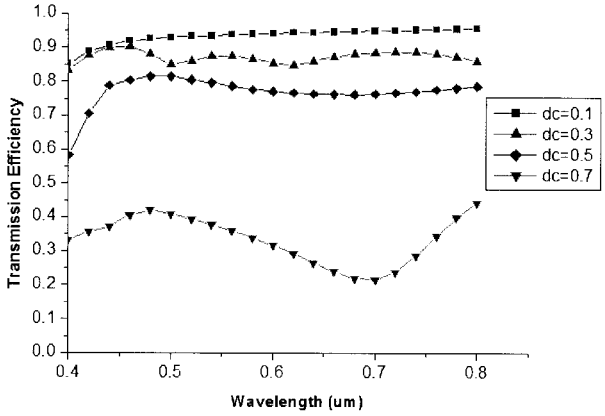

Fig. 5. Transmission efficiency of p-polarized light as a function of wavelength at various duty cycles (dc) of the multilayer grating. The period of an Al–SiO_2 grating was 0.2 μm. The thicknesses of the Al and the SiO_2 layers were 100 and 200 nm, respectively.

length grating was designed to operate in visible light. The diffraction efficiency was generally high in the red- and green-light wavelength spectra. For the blue-light spectrum the diffraction efficiency decreased rapidly at resonance wavelength λ, as determined by

$$\lambda = p(n_s \pm \sin\theta)/m, \tag{3}$$

where p is the period of the grating, n_s is the refractive index of the structure, and θ and m are the incident angle and the diffraction order, respectively. Low efficiency in the blue-light wavelength results in a narrowband spectrum that accompanies obvious color changes of the image for LCD applications. The limitation was overcome by the designed multilayer structure. The effective refractive index of a multilayer structure is an average value of refractive indices of dielectric layer and air spacing, which is lower than the refractive index of the substrate. Thus the effective refractive index of a multilayer structure is lower than that of a single layer. A lower effective refractive index shifts the resonance wavelength toward a shorter wavelength. The theoretical efficiency of the diffracted orders of the multilayer structures was calculated with the commercial software Grating Solver,[9] which uses rigorous coupled-wave analysis to yield the diffraction efficiencies and allows the complex refractive indices of the materials to be input.

The subwavelength grating was simulated for transmission of p-polarized light and reflection of s-polarized light. However, the transmission spectrum decreased abruptly at shorter wavelengths. A multilayer structure was then proposed to reduce the effective index of the structure, thereby lowering the resonance wavelength. Various materials for an additional dielectric layer (shown in Fig. 4), duty cycle (shown in Fig. 5), and thickness were simulated. Al (100 nm thick) and SiO_2 (200 nm thick) with a 0.2-μm period 50% duty cycle were eventually chosen for because of their ease of use and high efficiency. Al and SiO_2 were easily etched and lifted off. Although other highly reflective metals, such as Ag, can substitute for Al without degrading polarization efficiency, they are more expensive. In terms of form-birefringence effects, p-polarized light exhibits high transmission, similar to a dielectric layer. In contrast, s-polarized light exhibits high reflection, similar to a metal layer. The simulated properties of the subwavelength grating are shown in Fig. 6 for two cases: for an Al layer only, shown by dashed curves, and for an Al–SiO_2 layer, shown by solid curves. The transmission of the p-polarized light shown by the dashed curve decreases rapidly at shorter wavelengths. The efficiency was further improved by the multilayer structure. As shown by a solid curve, the transmission of p-polarized light is

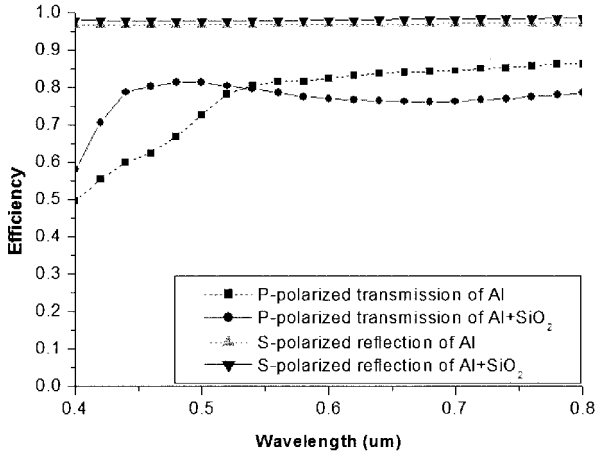

Fig. 6. p-polarized light transmission and s-polarized light reflection efficiencies of the subwavelength grating as functions of wavelength. The subwavelength grating retains high reflection efficiency for s-polarized light and high transmission efficiency for p-polarized light in the entire visible spectrum.

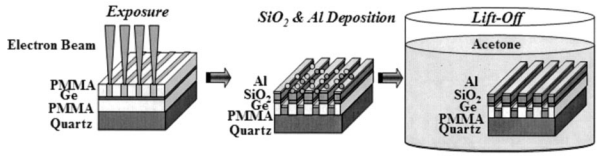

Fig. 7. Fabrication of the subwavelength grating. E-beam lithography and a lift-off method were used to fabricate the multilayered subwavelength grating.

~80% over the entire visible spectrum, whereas the reflection of *s*-polarized light is greater than 95%.

3. Fabrication

Two different structures, subwavelength grating and microslots, were fabricated individually on the top and bottom planes of the light guide. First, for microslot structures the slot patterns were fabricated by photolithography. A subwavelength grating was then fabricated as shown in Fig. 7.[10,11] First, 0.3-μm poly(methyl methacrylate) (PMMA), 0.03-μm Ge, and 0.3 μm PMMA were spin coated and sputtered in that order onto a quartz substrate to form a shadow mask and a conducting layer. *E*-beam lithography was then used to define a high-resolution grating with a period of 0.2 μm and a duty cycle of 50% over an 80 μm × 80 μm area, limited by the *E* beam used. After development, 0.2 and 0.1 μm of SiO_2 and Al were deposited sequentially. Finally, the PMMA pattern was lifted off in acetone to yield the subwavelength grating shown in Fig. 8. Electroplating and stamp molding were then applied to duplicate integrated light guides upon a plastic substrate.

4. Measurement

The transmission and reflection of the fabricated subwavelength grating were measured with a white-light source filtered with red (630-nm), green (532-nm), and blue (437-nm) primary wavelength color filters. The beam was focused onto the fabricated subwavelength grating (80 μm × 80 μm), and its input polarization was controlled by a polarization rotator. Two photodetectors were then used to measure the transmission and the reflection simultaneously. The measured and simulated reflection efficiencies are shown versus wavelength in Fig. 9. In such an arrangement the measured reflection efficiencies at λ = 437, 532, and 630 nm were 70%, 76%, and 85% for *s*-polarized light; transmission efficiencies for *p*-polarized light were 68%, 65%, and 70%, respectively.

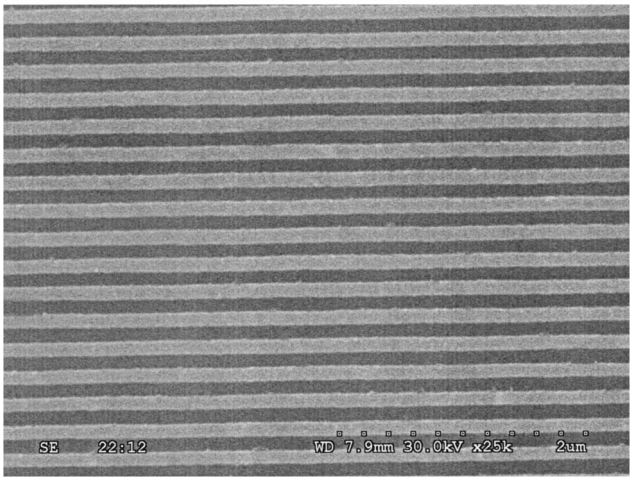

Fig. 8. Scanning-electron microscope photograph of the subwavelength grating with a period of 0.2 μm and a duty cycle of 50%.

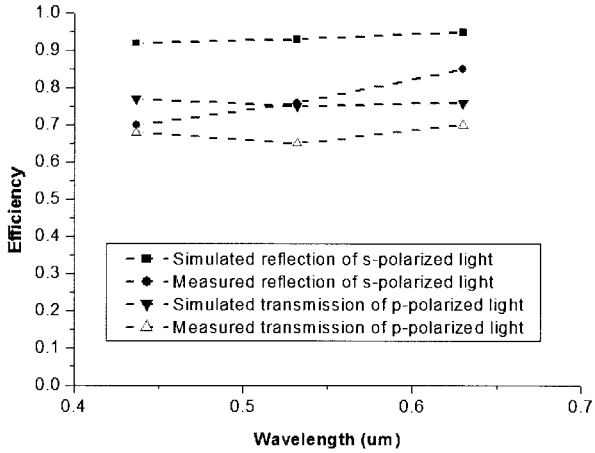

Fig. 9. Comparison of experimental and simulated results from the subwavelength grating. For measurements at λ = 437, 532, 630 nm the reflection efficiencies were 70%, 76%, and 85% for *s*-polarized light and 32%, 35%, and 30% for *p*-polarized light, respectively.

5. Discussion

Theoretically, a polarization-efficiency gain factor of 2 can be achieved. In the simulation the transmitted *p*-polarized light was P_{trans} + (*s* convert to *p*)$_{\text{trans}}$ = 80% × 0.5 + 95% × 0.5 × 0.9(quarter-wave plate conversion factor) × 80% = 75%. For conventional polarizers the transmitted *p*-polarized light is ~40%. Therefore the polarization-efficiency gain factor was 1.87. The difference in gain factor between theoretical and simulated values was attributed to differences in absorption of the materials. From the simulated results shown in Fig. 5 we found that the gain factor can be closer to the theoretical value of 2 if the linewidth of the subwavelength grating can be further reduced. In our measurement the transmitted *p*-polarized light was 85% × 0.5 + 70% × 0.5 × 0.9(quarter-wave plate conversion factor) × 85% = 69%. The measured results demonstrated that the gain factor of 1.7 was retained. Degradation of the gain factor was caused by several factors, described as follows: A Gaussian distribution of the *E* beam yielded a nonrectangular grating structure instead of a binary shape, lowering the efficiency of the total transmitted *p*-polarized light. A uniform beam profile could be obtained by use of electromagnetic lenses and smaller apertures to correct the Gaussian beam profile. Grating structures with

high aspect ratios could also reduce the effects of a nonrectangular shape. Moreover, the polarization efficiency was affected by the shape, linewidth, and layer thickness of the grating.[8] From measurement with an atomic-force microscope, the lateral and vertical errors of the subwavelength grating were 5% and 9%, respectively. We expect that more-precise lift-off and etching techniques will further improve the efficiency. Additionally, depolarization arose under conditions of mixed polarized states. With a 0.1-μm linewidth, the extinction ratio of *s*-polarized to *p*-polarized light exceeded 10. Although the extinction ratio was not so high, energy absorption was much reduced while the polarized light guide was illuminated on the liquid-crystal display panel. Theoretically, an extinction ratio of better than 25 could be achieved if the linewidth were further reduced. In the future a subwavelength grating of large area should be achievable by tiling of small-area grating arrays or use of nanoimprinting technology.[12]

6. Conclusions

An integrated light guide for liquid-crystal display illumination was developed with *p*-to-*s* polarization conversion and improved uniformity. This novel element combines microslot structures and a subwavelength grating on both surfaces of the light guide. An integrated polarized light guide was fabricated and evaluated for its functionality; we achieved 80% brightness uniformity and 69% polarization efficiency. Thus a gain factor of 1.7 in polarization efficiency was achieved. In addition, the extinction ratio of *s*-polarized to *p*-polarized light exceeded 10. Consequently, an integrated lightguide of high polarization conversion efficiency will provide a high-efficiency backlight module in compact form for LCD illumination.

This research was supported by the National Science Council of the Republic of China under contract NSC 91-2623-7-009-013. The authors acknowledge utilization of the fabrication and measurement systems of the Precision Instrument Development Center of the National Science Council and the National Changhua University of Education. In addition, the authors express their appreciation to Shr-Jia Shiu for assisting in the grating fabrication and to J. C. Wu and Hui-Hsiung Lin for valuable discussions.

References

1. W. A. Shurcliff, *Polarized Light* (Harvard U. Press, Cambridge, Mass., 1962).
2. S. M. P. Blom, H. P. M. Huck, H. J. Cornelissen, and H. Greiner, "Towards a polarized light emitting backlight: micro-structured anisotropic layers," SID J. **10,** 209–213 (2002).
3. M. F. Weber, "Retroreflecting sheet polarizer," in *Society of Information Display International Symposium Digest* (Society of Information Display, Boston, Mass., 1992), pp. 427–429.
4. K. W. Chien and H. P. D. Shieh, "An integrated lightguide equipped with polarization conversion," in *Society of Information Display International Symposium Digest* (Society of Information Display, Boston, Mass., 2002), pp. 1229–1231.
5. H. J. B. Jagt, H. J. Cornelissen, D. J. Broer, and C. W. M. Bastiaansen, "Linearly polarized light emitting backlight," in *International Display Workshops Digest* (Society of Information Display, Boston, Mass., 2000), pp. 387–389.
6. A. Yariv and P. Yeh, *Optical Waves in Crystal* (Wiley, New York, 1984).
7. F. Flory, L. Escoubas, and B. Lazarides, "Artificial anisotropy and polarizing filters," Appl. Opt. **41,** 3332–3335 (2002).
8. L. L. Soares and L. Cescato, "Metallized photoresist grating as a polarizing beam splitter," Appl. Opt. **40,** 5906–5910 (2001).
9. M. G. Moharam and T. K. Gaylord, "Diffraction analysis of dielectric surface-relief gratings," J. Opt. Soc. Am. **72,** 1385–1388 (1982).
10. J. C. Wu, M. N. Wybourne, W. Yindeepol, A. Weisshaar, and S. M. Goodnick, "Interference phenomena due to a double bend in a quantum wire," Appl. Phys. Lett. **59,** 102–104 (1991).
11. R. C. Tyan, A. A. Salvekar, H. P. Chou, C. C. Cheng, A. Scherer, and Y. Fainman, "Design, fabrication, and characterization of form-birefringent multilayer polarization beam splitter," J. Opt. Soc. Am. **14,** 1627–1636 (1997).
12. S. K. Moore, "Imprint lithography for nano-components," IEEE Spectrum **39**(5), 25–27 (2002).